REPORT DOCUMENTATION PAGE

Form Approved OMB NO. 0704-0188

1. REPORT DATE (DD-MM-YYYY)	2. REPORT TYPE	3. DATES COVERED (From - To)
11-02-2015	Final Report	19-May-2011 - 18-Nov-2014

4. TITLE AND SUBTITLE
Final Report: Development of Optical Crystals for High Power and Tunable Visible and Infrared Light Generation

5a. CONTRACT NUMBER
W911NF-11-1-0196

5b. GRANT NUMBER

5c. PROGRAM ELEMENT NUMBER
206022

6. AUTHORS
Arnold Burger

5d. PROJECT NUMBER

5e. TASK NUMBER

5f. WORK UNIT NUMBER

7. PERFORMING ORGANIZATION NAMES AND ADDRESSES
Fisk University
1000 17th Avenue North

Nashville, TN 37208 -3045

8. PERFORMING ORGANIZATION REPORT NUMBER

9. SPONSORING/MONITORING AGENCY NAME(S) AND ADDRESS (ES)
U.S. Army Research Office
P.O. Box 12211
Research Triangle Park, NC 27709-2211

10. SPONSOR/MONITOR'S ACRONYM(S)
ARO

11. SPONSOR/MONITOR'S REPORT NUMBER(S)
58976-PH-REP.5

12. DISTRIBUTION AVAILIBILITY STATEMENT
Approved for Public Release; Distribution Unlimited

13. SUPPLEMENTARY NOTES
The views, opinions and/or findings contained in this report are those of the author(s) and should not contrued as an official Department of the Army position, policy or decision, unless so designated by other documentation.

14. ABSTRACT
Lithium based chalcogenides 6LiInSe2 semiconductor has recently get much attention due to its possible application in neutron detection. It has a high resistivity and wide band gap 2.8 eV which makes it an attractive candidate for semiconductor radiation detector. Due to high reactivity of Li, stoichiometric amount of starting materials are grown as a red crystal with an absorption edge around 2.2 eV due to the intrinsic defect induced donor acceptor pair recombination. In this investigation we have introduced excess Li from stoichiometry 4% during synthesis of the 6LiInSe2 Charge materials with an intention to greenish yellow crystal by reducing the intrinsic

15. SUBJECT TERMS
Final Progress Report

16. SECURITY CLASSIFICATION OF:			17. LIMITATION OF ABSTRACT	15. NUMBER OF PAGES	19a. NAME OF RESPONSIBLE PERSON
a. REPORT	b. ABSTRACT	c. THIS PAGE			Arnold Burger
UU	UU	UU	UU		19b. TELEPHONE NUMBER 615-329-8516

Report Title

Final Report: Development of Optical Crystals for High Power and Tunable Visible and Infrared Light Generation

ABSTRACT

Lithium based chalcogenides 6LiInSe2 semiconductor has recently get much attention due to its possible application in neutron detection. It has a high resistivity and wide band gap 2.8 eV which makes it an attractive candidate for semiconductor radiation detector. Due to high reactivity of Li, stoichiometric amount of starting materials are grown as a red crystal with an absorption edge around 2.2 eV due to the intrinsic defect induced donor acceptor pair recombination. In this investigation we have introduced excess Li from stoichiometry 4% during synthesis of the 6LiInSe2 Charge materials with an intention to greenish yellow crystal by reducing the intrinsic defects. This award has extended our experimental capabilities and enabled us to consolidate past strengths to allow us to perform state-of-the-art research in the area of nonlinear optical crystals. These classes of infrared materials have high second and third order optical nonlinearities which are essential for second harmonic generation, optical parametric oscillation, optical switching, and wavelength conversion. In spite of being known and studied for a long period of time, the knowledge of the properties, figures-of-merit and ultimately their incorporation in useful devices has been hampered by compositional variations due to a combination of stoichiometry and extrinsic impurities. These characterization techniques are infrared absorption and Raman microscopy, emission spectroscopy, differential scanning calorimetry/thermogravimetric analysis, measurements of thermal diffusivity, scanning electron microscopy/energy dispersive X-ray analysis, atomic force microscopy and electrical charge carrier transport studies. We are focusing on the purification and growth of crystals belonging to the class of materials of the type Li-III-VI2 . We intend to achieve improvements through better purification and stoichiometry control during the crystal growth process.

Enter List of papers submitted or published that acknowledge ARO support from the start of the project to the date of this printing. List the papers, including journal references, in the following categories:

(a) Papers published in peer-reviewed journals (N/A for none)

Received		Paper
02/11/2015	4.00	V. Buliga, M. Groza, B. Wiggins, A. Burger, A. Stowe, Y. Cui, E. Tupitsyn, P. Bhattacharya, E. Rowe, L. Matei. Lithium containing chalcogenide single crystals for neutron detection, Journal of Crystal Growth, (05 2014): 0. doi: 10.1016/j.jcrysgro.2013.10.054
08/25/2014	3.00	Pijush Bhattacharya, Vladimir Buliga, Yunlong Cui, Eugene Tupitsyn, Emmanuel Rowe, Brenden Wiggins, Daniel Johnstone, Ashley Stowe, Arnold Burger. Defects in 6LiInSe2 neutron detector investigated by photo-induced current transient spectroscopy and photoluminescence, Applied Physics Letters, (08 2013): 0. doi: 10.1063/1.4819733
TOTAL:	**2**	

Number of Papers published in peer-reviewed journals:

(b) Papers published in non-peer-reviewed journals (N/A for none)

Received Paper

TOTAL:

Number of Papers published in non peer-reviewed journals:

(c) Presentations

Number of Presentations: 1.00

Non Peer-Reviewed Conference Proceeding publications (other than abstracts):

Received Paper

TOTAL:

Number of Non Peer-Reviewed Conference Proceeding publications (other than abstracts):

Peer-Reviewed Conference Proceeding publications (other than abstracts):

Received Paper

TOTAL:

Number of Peer-Reviewed Conference Proceeding publications (other than abstracts):

(d) Manuscripts

Received Paper

TOTAL:

Number of Manuscripts:

Books

Received Book

TOTAL:

Received Book Chapter

TOTAL:

Patents Submitted

Patents Awarded

Awards

Graduate Students

NAME	PERCENT_SUPPORTED	Discipline
Jonathan Florez	0.75	
Joanna Egner	0.75	
Joseph Bell	0.75	
Ardelia Clark	0.75	
Jodie Hawk	0.50	
FTE Equivalent:	**3.50**	
Total Number:	**5**	

Names of Post Doctorates

NAME	PERCENT_SUPPORTED
FTE Equivalent:	
Total Number:	

Names of Faculty Supported

NAME	PERCENT_SUPPORTED	National Academy Member
Arnold Burger	0.02	
FTE Equivalent:	**0.02**	
Total Number:	**1**	

Names of Under Graduate students supported

NAME	PERCENT_SUPPORTED
FTE Equivalent:	
Total Number:	

Student Metrics

This section only applies to graduating undergraduates supported by this agreement in this reporting period

The number of undergraduates funded by this agreement who graduated during this period:	0.00
The number of undergraduates funded by this agreement who graduated during this period with a degree in science, mathematics, engineering, or technology fields:	0.00
The number of undergraduates funded by your agreement who graduated during this period and will continue to pursue a graduate or Ph.D. degree in science, mathematics, engineering, or technology fields:	0.00
Number of graduating undergraduates who achieved a 3.5 GPA to 4.0 (4.0 max scale):	0.00
Number of graduating undergraduates funded by a DoD funded Center of Excellence grant for Education, Research and Engineering:	0.00
The number of undergraduates funded by your agreement who graduated during this period and intend to work for the Department of Defense	0.00
The number of undergraduates funded by your agreement who graduated during this period and will receive scholarships or fellowships for further studies in science, mathematics, engineering or technology fields:	0.00

Names of Personnel receiving masters degrees

NAME
Total Number:

Names of personnel receiving PHDs

NAME
Total Number:

Names of other research staff

NAME	PERCENT_SUPPORTED
Constantine Coca	0.04
Hugo Espejel	0.16
Terreka Hart	0.21
FTE Equivalent:	**0.41**
Total Number:	**3**

Sub Contractors (DD882)

Inventions (DD882)

Scientific Progress

In this project we have demonstrated the synthesis and crystal growth of an important nonlinear optical material, LiInSe2. Compared with the results published in the literature by other groups the crystals grown at Fisk have the lowest defect content, a property that is fundamental to high powers laser applications where residual impurities cause detrimental optical losses. The main approaches for this improvements were: (i) the use of high purity lithium (5N), (ii) a two-step synthesis preventing contamination during synthesis, and (iii) use of Li (1-2%) and Se (1-2%) excess during growth to compensate for the loss of lithium and selenium which are the volatile components of LiInSe2.

Technology Transfer

Department of Defense (DoD) Program of Research and Educational Program for Historically Black Colleges and Universities and Minority-Serving Institution (HBCU/MSI)

Grant Number: W911NF-11-1-0196
Fisk Grant #: 2509
Proposal # 58976-PH-REP
Project Title: "Development of Optical Crystals for High Power and Tunable Visible and Infrared Light Generation"

Author of Report:
Arnold Burger
Phone: (615) 329-8516;
Fax: (615) 329-8634;
E-mail: aburger@fisk.edu

Performing Organization Name(s) and Address(es):
Fisk University,
Department of Physics,
1000 17th Avenue North,
Nashville, TN 37208

Final Report for the Period of Performance: 19 May 2011 - 18 November 2014
Award Amount: $575,000.00
PI: Arnold Burger, Ph.D.

ARO Grants Officer's Representative is Dr. Richard Hammond, (919) 549-4313,
email: richard.hammond@us.army.mil
Co-Grants Officer's Representative is Dr. Howard Schlossberg, (703) 696-7549,
email: howard.schlossberg@afosr.af.mil

Summary

Lithium based chalcogenides 6LiInSe2 semiconductor has recently get much attention due to its possible application in neutron detection. It has a high resistivity and wide band gap 2.8 eV which makes it an attractive candidate for semiconductor radiation detector. Due to high reactivity of Li, stoichiometric amount of starting materials are grown as a red crystal with an absorption edge around 2.2 eV due to the intrinsic defect induced donor acceptor pair recombination. In this investigation we have introduced excess Li from stoichiometry 4% during synthesis of the 6LiInSe2 Charge materials with an intention to greenish yellow crystal by reducing the intrinsic defects. This award has extended our experimental capabilities and enabled us to consolidate past strengths to allow us to perform state-of-the-art research in the area of nonlinear optical crystals. These classes of infrared materials have high second and third order optical nonlinearities which are essential for second harmonic generation, optical parametric oscillation, optical switching, and wavelength conversion. In spite of being known and studied for a long period of time, the knowledge of the properties, figures-of-merit and ultimately their incorporation in useful devices has been hampered by compositional variations due to a combination of stoichiometry and extrinsic impurities. These characterization techniques are infrared absorption and Raman microscopy, emission spectroscopy, differential scanning calorimetry/thermogravimetric analysis, measurements of thermal diffusivity, scanning electron microscopy/energy dispersive X-ray analysis, atomic force microscopy and electrical charge carrier transport studies. We are focusing on the purification and growth of crystals belonging to the class of materials of the type Li-III-VI_2 . We intend to achieve improvements through better purification and stoichiometry control during the crystal growth process.

Technical Report

For the implementation of bulk solid state detection devices, the crystal growth procedure must be optimized and standardized to produce large ingots. The growth of I-III-VI_2 compounds including $LiInSe_2$ have been extensively studied for non-linear optical applications such as second harmonic generation.[1][2][3] We report on the synthesis and growth procedures under various conditions are presented and compared. Optical properties were studies by absorption spectroscopy in the visible a, near-infrared and in the mid-infrared. Samples were characterized by temperature dependent optical absorption spectroscopy. Macroscopic properties were tested for samples of varying stoichiometric weight ratios. The resistivity of $^6LiInSe_2$ crystals was found in the range of 1-3 $x10^{12}$ ohm-cm with having a significant effect of excess Li concentrations.

1) Synthesis and Crystal Growth

Chemical purity is vital to synthesis of a single phase ternary semiconductor and subsequent growth of large bulk crystals. As such, indium (6N) and selenium (5N) were used from commercial sources. Li, however, is not commercially available with high chemical purity, especially when isotopically enriched to ^6Li. To achieve ultra high chemical purity (5N), 95% isotopically enriched ^6Li was purified in a multi-stage vacuum distillation process previously reported by Stowe *et al.*[4]. ^6LiIn alloy was synthesized in a separate step prior to selenium addition in order to control ^6Li stoichiometry [5]. ^6LiIn and $^6LiInSe_2$ were synthesized in a pyrolotic boron nitride (PBN) crucible to maximize chemical compatibility with the constituent elements. Lithium is highly reactive metal and to overcome this problem and create the stoichiometric composition of I-III-VI_2 in two steps:

- 1 : Li+In metal alloy
- 2 : LiIn+Se using vapor transport of Se

A typical charge of the synthesized LiInSe2 is shown in Figure 1 below.

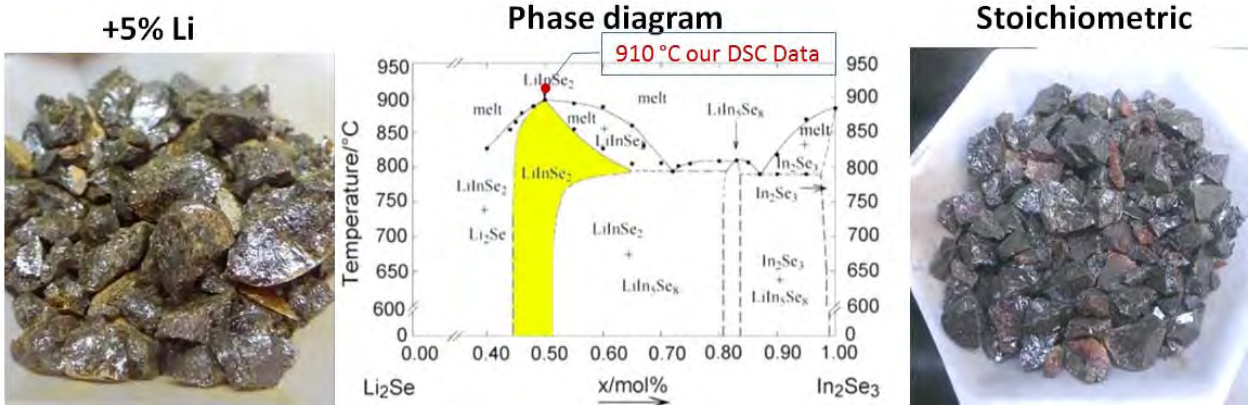

Figure 1. The synthesized LiInSe2 charge of the ternary compound to be used for growth (left, using 5% Li excess, right, under stoichiometric conditions. The phase diagram of the pseudobinary Li_2Se – In_2Se3 is also shown *[WEISE, KRÄMER: Li_2Se–In_2Se3; JTAC#71, 2003]*

The ternary synthesized material was then loaded into another PBN crucible and sealed in a quartz ampoule under argon pressure of 0.5 atm. Growth was carried out in a two zone vertical Bridgman furnace.

The vertical Bridgman apparatus utilized resistive coils, in temperature controlled zones, in a practically thermally isolated enclosure, as shown in Figure 2. The hot zone was set at a temperature of 950^{o}C and the cold zone was set at 750^{o}C. The vertical growth translation rate was 0.5 - 1cm/day. The as-grown crystal ingot exhibited variation in color along the growth axis and radially along cut planes.

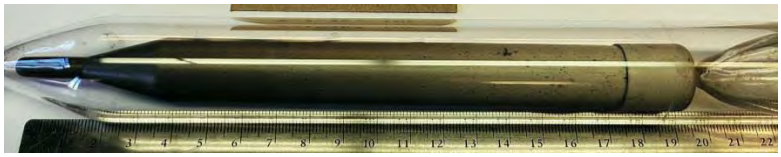

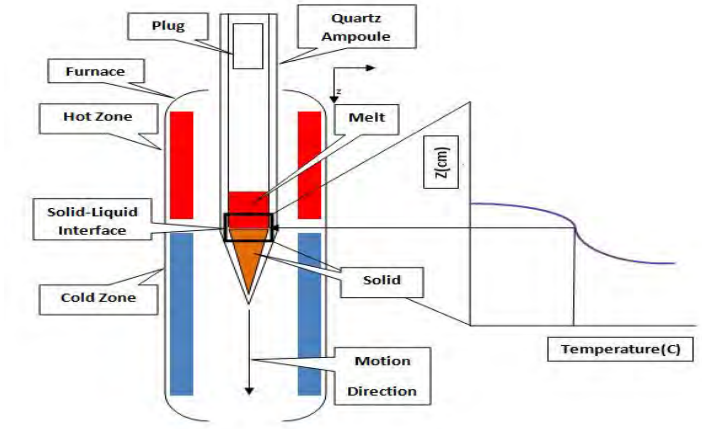

Figure 2. Photos of a two-zone furnace with spatially static thermal gradient. The setup was equipped with a stepper motor allowing to rotate the ampule the option for using the Accelerated Crucible Rotation Technique (ACRT). ACRT allows agitation and better mixing of melt using

intermittent rotation. The fused silica ampule containing the pBN crucible is shown to the right. Chemical purity is vital to synthesis of a single phase ternary semiconductor and subsequent growth of large bulk crystals. As such, indium (6N) and selenium (5N) were used from commercial sources. Li, however, is not commercially available with high chemical purity, especially when isotopically enriched to ^{6}Li. To achieve ultra high chemical purity (5N), 95% isotopically enriched ^{6}Li was purified in a multi-stage vacuum distillation process previously reported by Stowe *et al.*[4]. ^{6}LiIn alloy was synthesized in a separate step prior to selenium addition in order to control ^{6}Li stoichiometry [5]. ^{6}LiIn and ^{6}LiInSe$_2$ were synthesized in a pyrolytic boron nitride (pBN) crucible to maximize chemical compatibility with the constituent elements. The ternary synthesized material was then loaded into another PBN crucible and sealed in a quartz ampoule under argon pressure of 0.5 atm. Growth was carried out in a two zone vertical Bridgman furnace. The vertical Bridgman apparatus utilized resistive coils, in temperature controlled zones, in a practically thermally isolated enclosure, as shown in Figure 2. The hot zone was set at a temperature of 950^{o}C and the cold zone was set at 750^{o}C. The vertical growth translation rate was 1cm/day. The as-grown crystal ingot exhibited variation in color along the growth axis and radially along cut planes.

After finishing the crystal growth representative cylindrical cross-section are then extracted from the ingot and then perpendicularly sliced into wafer cross-sections, as presented in Figures 3 and 4.

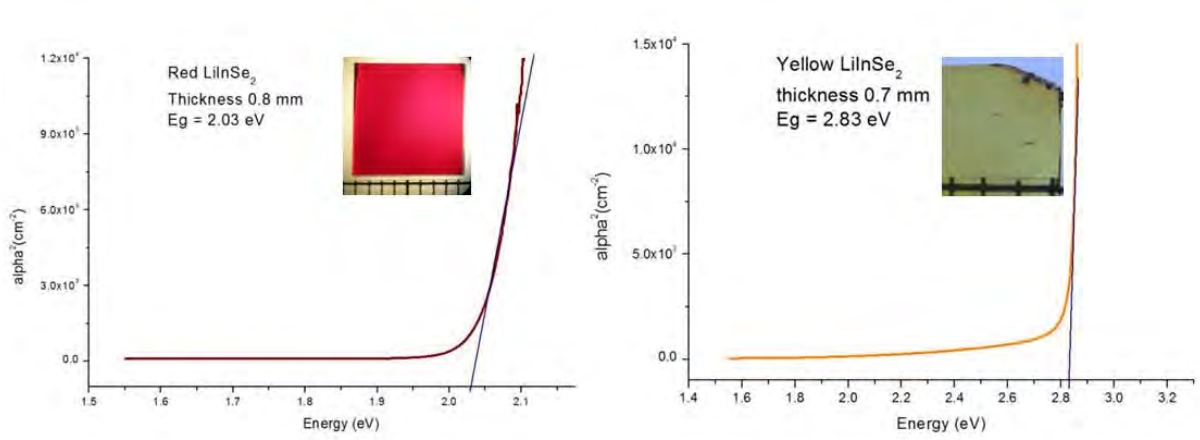

Figure 3 Photo of a representative sample section illuminated by transmission exhibiting "red" and "yellow" regions. The absorption tail of red crystals at 2.03 eV (left) is explained by lithium vacancies defects. Crystals grown under excess lithium) yellow crystal shown to the right_ display the proper absorption spectrum characteristic of the banndgap of 2.81eV for LiInSe$_2$

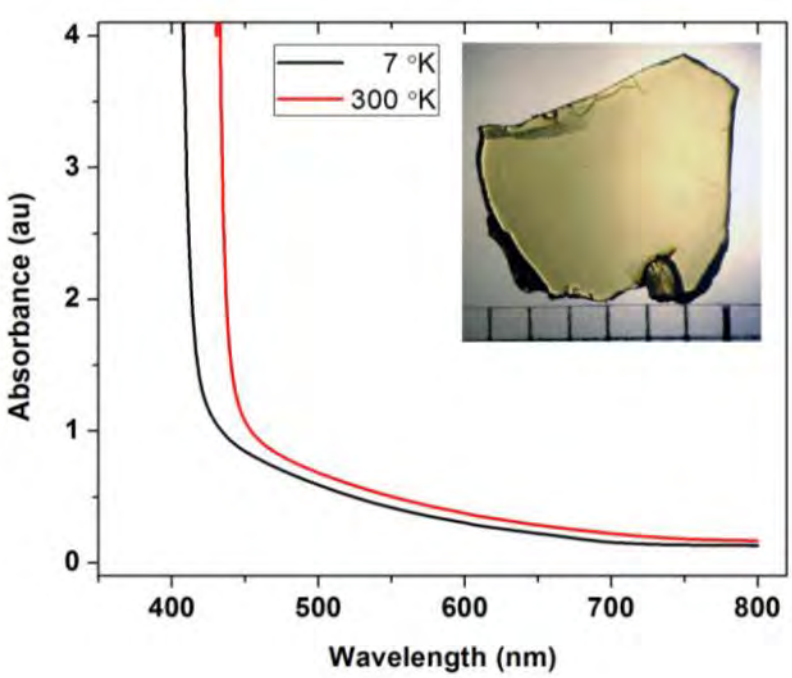

Figure 4. Absorption spectrum of LiInSe2 (yellow) at room temperature (300K) and at 7 K. The sample thickness was 0.5 mm.

However, synthesis and growth of these I-III-VI_2 compounds possess intrinsic complexities in obtaining large bulk crystals with material uniformity and purity including the corrosive nature of lithium and a relatively high vapor pressure of lithium and selenium.[6] The conditions of growth of these compounds by melt solidification must therefore be selected to overcome the preferential evaporation of constituent material, as reported previously [7]. The utilization of boron nitride crucibles have been shown to provide good chemical compatibility and thermal stability with the handling of lithium compounds.[8] Visible inclusions have also been reported in as-grown $LiInSe_2$ ingots.[9] Non-uniform material distribution, precipitation and inclusions can affect the electrical properties with the production of charge carrier traps within the $LiInSe_2$ matrix and non-uniformity in the internal electric field. In the present study, impurity concentrations as well as the distribution of constituent I-III-VI_2 elements in as-grown $LiInSe_2$ samples have been investigated with IR microscopy and laser induced breakdown spectroscopy (LIBS) to understand potential charge trapping sites and aid in the improvement of synthesis, purification and growth procedures.

Specific inclusions have been identified within the $^{6}LiInSe_2$ matrix using laser induced breakdown spectroscopy performed on our samples by our collaborator at Y-12 National Security Complex. The inclusions consist of calcium, sodium and potassium. All impurities are concentrated in the red region of the crystal which has poor performance. It is likely that these impurities act as point defects and charge trapping sites, which can hindering charge carrier transport in the crystal. Further, examination of constituent host material stoichiometry ratios reveals spatial inhomogeneity across the interrogated region of the crystal. Assuming that the yellow crystal has ideal stoichiometry, the preferential loss of Se and higher content of Li and In also promotes the formation of a red crystal. Excess lithium and indium in this red color region can led to interstitial

sites causing charge (hole) trapping during photo-ionization or neutron radiation detection. A plausible explanation is that the color differences are cause by point defects generated by the coupled effect of the presence of both impurities and deviation from stoichiomentry.

2) Electrical measurements using current-voltage characteristics

In this section, we will discuss the electrical measurements performed on the LiInSe2 samples $LiInSe_2$ wafers from each growth run are polished, etched in 5% Br: Methanol for 1 minute and then gold contacts were deposited using sputtering on both sides of the wafer for electrical measurements. Resistivity of the wafers was found to be approximately $6.5x10^{10}$ ohm-cm
I-V characteristics and photoconductivity spectra of LiInSe2 are shown in Figure 5.

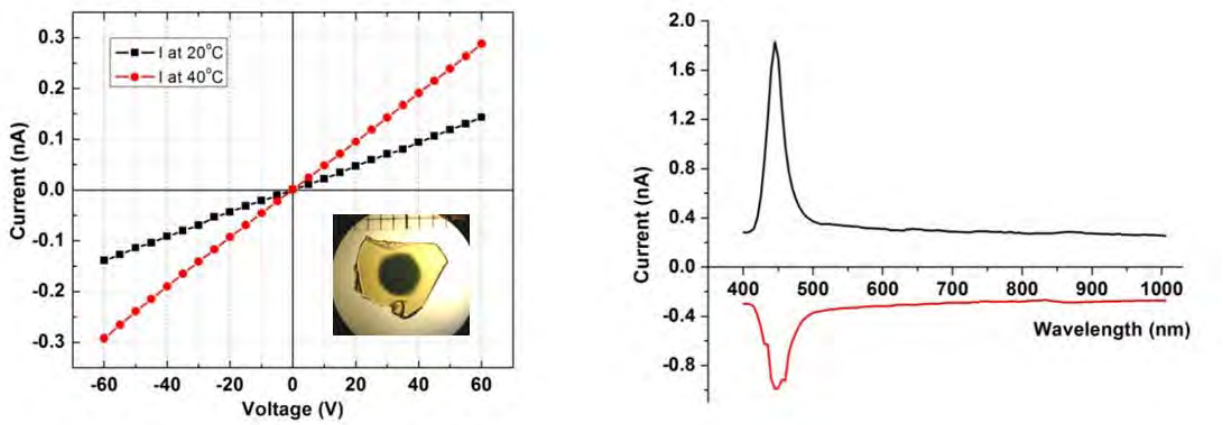

Figure 5 Current-voltage characteristic of LiInSe2 at 20 °C and 40 °C (left); sample thickness is 0.5 mm contact diameter is 3.2 mm; The resistivity values extracted are $\rho 20\ °C = 6.5\times10^{11}\ \Omega\cdot cm$, and $\rho 40\ °C = 3.17\times1011\ \Omega\cdot cm$; The photoconductivity spectrum of $LiInSe_2$ (right) ; Sample thickness is 0.5 mm and gold contact diameter is 3.2 mm; Bias is -60 V for black (top) curve (cathode was illuminated) and +60 V for red (bottom) curve (anode was illuminated).

1) Optical Absorbance in the visible and near-infrared

In this section, we will discuss the principles of optical characterization and the macroscopic quantities extracted from this technique. Within the framework of quantum mechanics, it has been determined that atoms, molecules, ions have discrete energy levels. Therefore there exists allowed atomic transitions unique to given species. Optical absorption is an experimental apparatus that measures the transfer of electromagnetic energy to a given species in the sample. Absorption events can excite electrons from its initial energy state to higher energy states. In this apparatus, the sample is irradiated with a varying monochromatic source normal to the surface (the initial intensity is measured respectfully), there a detector setup collects the remaining photons and measures the transmitted intensity. This allows us to observe the measurable quantity called absorbance given by:

$$A = \log_{10} \frac{I_0}{I} \tag{1}$$

Where A is Absorbance, I_0 is the initial intensity and I is the transmitted intensity. If we assume the transmitted intensity takes the form below:

$$I = I_0 e^{-\alpha t} \tag{2}$$

We may also readily extract the linear attenuation coefficient given by:

$$\alpha = \frac{(2.303 * A)}{t} \tag{3}$$

Where t is the thickness of the sample and is the α linear attenuation coefficient. The assumption of (3) does not consider the loss of initial intensity by reflection at the surface or scattering at either end of the sample. To minimize scattering at the surface, the sample goes through a procedural polishing elaborated in the fabrication section.

This experimental process can excite electrons in foreign species in the material (assuming the energy of the source is near the magnitude of an allowed absorption transition of the impurity species) or elevates electrons from the valence band into the conduction band producing electron hole pairs (under the condition that the energy of the source is equal to or higher than the band gap of the material). If the energy of the source is lower than the band gap of the material then the electron does not have enough energy to be promoted to the conduction band. The energy interval corresponding to the transition of non-absorbing to absorbing is defined as the absorption edge. This corresponds to band gap of the material. In this energy interval of the source, the photons have a higher probability of being absorbed by the electrons and promoted to the conduction band. This increases the number of photons absorbed in the material.

Direct band gap semiconductors obey the relation given by:

$$\alpha = C * (h\nu - E_g)^{\frac{1}{2}} \tag{4}$$

where C is an characteristic constant, h is Planck's constant, E_g is the band gap of the material, ν is the frequency of the source. With this relation we are able to extract the band gap from the independent axis intercept of the α^2 vs. $h\nu$ plot by linear extrapolation of the curve above the absorption edge, as shown in Figure 3.

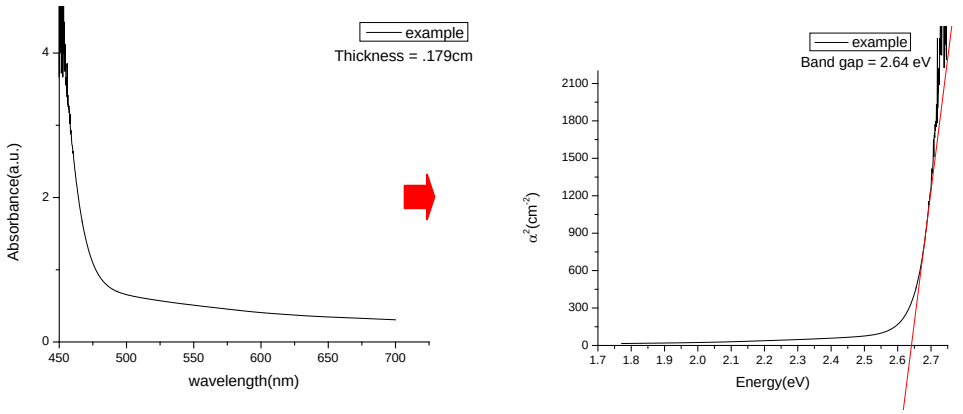

Figure 3 Illustration of band gap determination of LiInSe2 by optical absorbance measurements. The spectra above were taken at room temperature.

An empirical expression describing the band gap as a function of temperature is given by Varshni's relation

$$E_g(T) = E_g(0) - \delta \frac{T^2}{T+\beta} \tag{5}$$

Where $E_g(0)$ is the reference band gap, $E_g(T)$ is the band gap corresponding to a temperature change, δ and β are arbitrary constants determined for the data. The apparatus is illustrated in figure 4. The temperature dependent band gap of the $LiInSe_2$ crystals were determined using optical absorption spectra measured by UV-Vis-NIR spectrophotometer (Varian Cary 500 Scan) coupled with a cryo-chamber, aperture, helium compressor and temperature controller. This measurement was taken in the temperature controlled cryo-chamber.

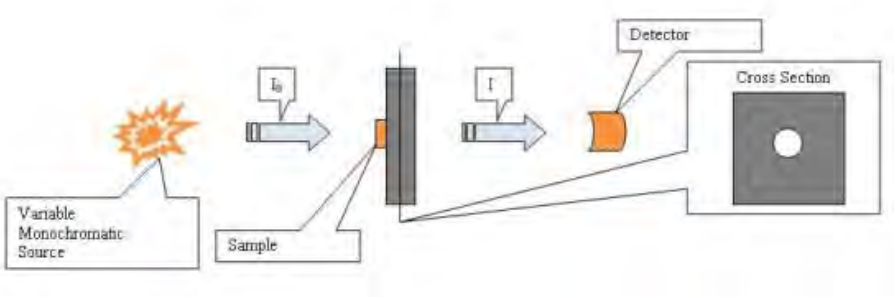

Figure 4 Illustration of the optical absorption apparatus

2) Fourier Transform Infrared Transmission (FTIR)

In this section, we will discuss the principles of FTIR Transmission. This technique also takes advantage of allow atomic transitions. The setup has similar applications as optical absorption, but has the ability to explore lower photon energy ranges. In this apparatus, the sample is irradiated with a modulated source, induce by the use of an interferometer, normal to the surface (the initial intensity is measured respectfully), there the detector setup collects the remaining photons of the polychromatic light and measures the transmitted intensity in each frequency utilizing the mathematical framework of Fourier analysis. This allows us to observe the measurable quantity called Transmittance given by (6):

$$T = \frac{I(v)}{I_0(v)} = e^{-\alpha t} \tag{6}$$

Here T is transmittance, I_0 is the initial Intensity, $I(v)$ is the modulated transmitted Intensity, and $I_0(v)$ is the modulated initial Intensity. The apparatus is illustrated in figure 11. FTIR Transmission was measured by a Bruker instrument model Tensor 27. The measurement was taken at room temperature in ambient environment.

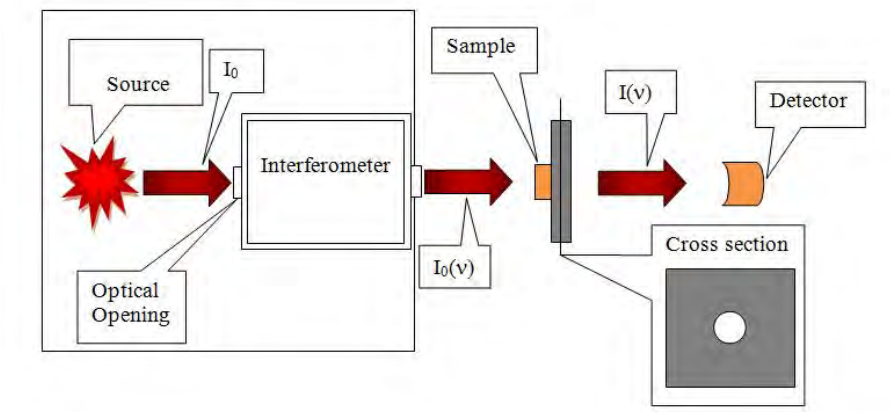

Figure 5 Illustration of the FTIR system.

3) Optical Absorption as a function of temperature

All optical measurements were taken with un-polarized light. Upon inspection of the α^2 vs. energy plot and by utilizing the framework built in the characterization section, one can observe the band gap as a function of temperature for the $LiInSe_2$ sample.

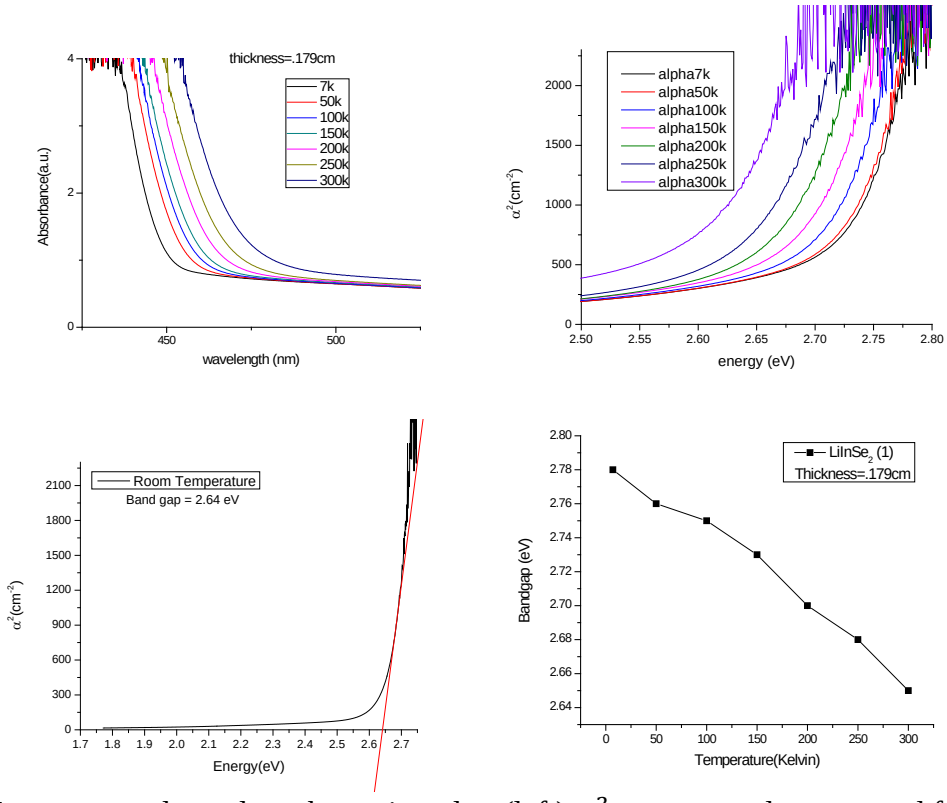

Figure 6 Temperature dependent absorption plot. (left) α^2vs. energy plot extracted from the optical absorption data.(right) band gap vs. temperature plot of the fabricated $LiInSe_2$ sample.(bottom right) α^2 vs. energy plot at room temperature (bottom left)

The band gap exhibits a linear relationship with temperature. Best linear fit yields a slope of $dEg/dT = -4.35519\times10^{-4}$ eV/K $\pm 2.4\times10^{-5}$eV/K. This value is slightly lower than the value obtained in [10]. The band gap at room temperature was measured to be 2.64 eV. The Varshni parameters are given in Table 1.

Table 1

Varshni parameter table	
δ	$5.8 \times 10^{-4}\ eV\ K^{-1} \pm 1.04 \times 10^{-4}\ eV\ K^{-1}$
β	$105.65\ K\ \pm 73.75\ K$
$E_g(0)$	$2.776\ eV \pm 4.66\ \times 10^{-3}\ eV$

Conclusions

Understanding the compositional variation and impurity distribution present in each portion or color of the $LiInSe_2$ crystal can therefore inform future synthesis and crystal growth optimization. These ratio maps could be an excellent component in the evaluation the spatial electrical properties and response of future detectors with stoichiometric variations. Annealing in vacuum or excess of one constituent element will be investigated in the next year to optimize crystal stoichiometry, improve uniformity and charge transport through the crystal, especially for larger crystal growth operations. In summary, Li containing semiconductor $LiInSe_2$ was successfully grown using the Bridgman technique.

We have been able to control the reactivity of lithium with the fused silica ampules and crucibles by using a two step synthesis. In the first step the intermetallic compound LiIn is obtained and the LiInSe2 compound is obtained in the vapor phase by reciting the LiIn with Selenium vapor. The color of the $LiInSe_2$ crystal grown with 5% excess lithium was yellow and band gap energy at room temperature was 2.8 eV in agreement with the previous reports. The crystal showed a high bulk resistivity of 6.5 x 10^{11} Ω·cm—suitable for high power laser applications.

The photocurrents are well pronounced at 445 nm and suggests good generation rate and mobility of the charge carriers. The $LiInSe_2$ crystal showed an excellent transparency for crystals prepared with an excess of Li that allows reducing the concentration of lithium vacancies that are typically obtained from growth experiments under stoichiometric conditions.

References

1. Isaenko, L.I., and Vasilyeva, I.G. (2008). Nonlinear $LiB^{III}C^{VI}_2$ crystals for mid-IR and far-IR: Novel aspects in crystal growth. *Journal of Crystal Growth*, 310, 1954-1960.
2. Isaenko, L., Vasilyeva, I., Merkulov, A., Yelisseyev, A., and Lobanov, S. (2005). Growth of new nonlinear crystals LiMX2 (M= Al, In, Ga; X=S, Se, Te) for the mid-IR optics. *Journal of Crystal Growth*, *275*, 217-223.
3. Isaenko, L., Yelisseyev, A., Lobanov, S., Krinitsin, P., Petrov, V., and Zondy, J.J. (2006). Ternary chalcogenides $LiBC_2$ (B=In, Ga; C=S,Se,Te) for mid-IR nonlinear optics. *Journal of Non-Crystalline Solids*, 352, 2439-2443.
4. Stowe, A. C., Morrell, J. S., Bhattacharya, P., Tupitsyn, E., Burger, A. (2011). Synthesis of a potential semiconductor neutron detector crystal $LiGa(Se/Te)_2$: Materials purity and compatibility effects. *Proc. of SPIE*, 8142, 8142H-1-8.
5. Tupitsyn, E., Bhattacharya, P., Rowe, E., Matei, L., Groza, M., Wiggins, B., Burger, A., and Stowe, A. (2012). Single crystal of $LiInSe_2$ semiconductor for neutron detector. *Journal of Applied Physics*, 101(12).
6. Kamijoh, T., and Kuriyama, K. (1981). Single Crystal Growth and Characterization of $LiInSe_2$. *Journal of Crystal Growth*, 51(1102), 6-10.Vasilyeva, I.G., Nikolaev, R.E., Malakhov, V.V., and Isaenko, L.I. (2007).
7. Effects of evaporation and melting on nonstoichiometry and inhomogeneity of $LiInSe_2$ crystals. *Journal of Thermal Analysis and Calorimetry*, 90(2), 601-605.
8. Jang, G.E., Curelaru, I.M., and Hentschel, M.P. (1994). Growth and characterization of large singe crystals of the intermetallic compound Li-Ga(Zintl). *Journal of Crystal Growth*, 141, 399-403.
9. Badikov, V.V., Chizhikov, V.I., Efimenko, V.V., Efimenko, T.D., Panyutin, V.L., Shevyrdyaeva, G.S., and Scherbakov, S.I. (2003). Optical properties of lithium indium selenide. *Optical Materials*, 23, 575-581.
10. Harig, W., Newmann, H., & Kuhn, G. (1983). The Fundamental Absorption Edge of $LiInSe_2$. *Phys. Status Solidi B*, 121, K55-K58.